20 October 2000

ELSEVIER

Chemical Physics Letters 329 (2000) 311–316

CHEMICAL PHYSICS LETTERS

www.elsevier.nl/locate/cplett

Quantum rotation of hydrogen in single-wall carbon nanotubes

C.M. Brown [a,b], T. Yildirim [b], D.A. Neumann [b,*], M.J. Heben [c], T. Gennett [c,e], A.C. Dillon [c], J.L. Alleman [c], J.E. Fischer [d]

[a] *Department of Materials and Nuclear Engineering, University of Maryland, College Park, MD 207421, USA*
[b] *National Institute of Standards and Technology, NIST Center for Neutron Research, Gaithersburg, MD 208991, USA*
[c] *Center for Basic Science, National Renewable Energy Laboratory, 1617 Cole Blvd., Golden, CO 80401, USA*
[d] *Department of Materials Science and Engineering, University of Pennsylvania, Philadelphia, PA 19104, USA*
[e] *Center for Materials Science and Engineering, Rochester Institute of Technology, Rochester, NY 14623, USA*

Received 11 July 2000

Abstract

We report inelastic neutron scattering results on hydrogen adsorbed onto samples containing single-wall carbon nanotubes. These materials have attracted considerable interest recently due to reports of high density hydrogen storage at room temperature. Inelastic neutron scattering clearly shows the *ortho–para* conversion of physisorbed hydrogen in a nanotube containing soot loaded with hydrogen. From the rotational $J = 0 \rightarrow 1$ transition, no indication of a significant barrier to quantum rotation is seen.

1. Introduction

It is desirable to develop hydrogen-based energy systems to alleviate environmental damage by reducing carbon dioxide generation and to prepare for projected petroleum shortages. However, advances in a variety of areas are necessary before hydrogen can be widely used as an energy carrier. Current hydrogen storage technologies, in particular, are inadequate in terms of gravimetric and volumetric storage densities, energy efficiency, safety, and cost. Therefore, hydrogen storage systems have been the focus of much recent research and development activity.

A safe, compact and inexpensive system capable of storing 6.5 wt% hydrogen without excessive heating, cooling, or pressurization would be of great interest [1]. Several recent investigations have reported that nanostructured carbon materials can exhibit such high storage densities at room temperature. Promising results have been reported for single-walled carbon nanotubes (SWNT) [1,2], alkali-doped vapor-grown carbon nanotubes (CNT) and graphite [3], as well as graphitic nanofibers (GNF) [4–6]. All these findings, however, remain quite controversial. For example, Dillon et al. [1] investigated impure SWNT samples at room temperature and 0.41 atm and determined that hydrogen storage densities would be between 5 and 10 wt% on pure samples, while Liu et al. [2]

* Corresponding author. Fax: 1-301-921-9847.
E-mail addresses: dan@nist.gov (D.A. Neumann), mikeheben@nrel.gov (M.J. Heben).

0009-2614/00/$ - see front matter
PII: S0009-2614(00)01003-4

measured 4.2 wt% storage at 10 MPa on purer samples. In contrast, Ye et al. [7] examined pure SWNTs and found a high density of 8 wt% (H/C ~1) only at 80 K and 100 atm. Alkali metal-doped CNTs were reported to store 14 and 20 wt% hydrogen by Chen et al. [3], but these findings could have been compromised by the presence of water [8]. GNFs have been reported to be tremendous adsorbents for hydrogen, storing 10–12 wt% at ~7–15 atm in one laboratory [6], and 30–50 wt% (H/C = 12) at 110 atm in another [4,5]. However, Ahn et al. [9] measured GNFs to adsorb only ~0.4 wt% hydrogen at 300 K and 160 bar, in similarity to most forms of carbon.

The interest in SWNTs, CNTs, and GNFs for hydrogen storage is based on the idea that the nanostructured environments present in these materials might afford unusually strong stabilization forces in comparison to more conventional adsorbents. Several theoretical efforts have attempted to describe the observations of hydrogen storage at room temperatures. For example, the interstitial sites between individual SWNTs in a bundle and also the central pore within a SWNT are predicted to be more effective than planar graphite in adsorbing H_2 [10], but no model has been able to account for interactions which would lead to the high amounts of hydrogen stored at room temperature [1,2] or the 19.6 kJ/mol heat of adsorption that has been reported [1]. The majority of experimental data has focused on capacity and charge/discharge behavior, and has not been of great use to theoreticians attempting to understand these observations. In fact, to the best of our knowledge no structural or spectroscopic in situ experimental results are available for any of these carbon-based hydrogen storage systems.

We have used the neutron scattering facilities at the NIST Center for Neutron Research, to structurally characterize our as-produced SWNT sample using the BT1 powder diffractometer [11], and then to probe the rotational potential felt by adsorbed hydrogen as a function of temperature with the BT4 filter–analyzer inelastic spectrometer [12]. In the solid, hydrogen behaves as a three-dimensional quantum rotor with energy levels given by $E_J = BJ(J+1)$, where J is the rotational quantum number and $B = 7.35$ meV is the rotational constant. Here we use the $J = 0 \rightarrow 1$, or *para* $\rightarrow$ *ortho* transition, as a probe of hydrogen binding sites. This transition occurs at an energy close to $2B = 14.7$ meV in the pure molecular solid because the molecules are essentially free quantum rotors with no center-of-mass translation. In the gas phase, the continuous spectrum of recoil energies broadens the rotational transition, so the technique is able to discern adsorbed molecules which do not diffuse. Relatively weak interactions between the rotating molecule and its environment will alter this simple energy level scheme; given sufficient spectroscopic resolution, one can deduce accurate information about the adsorbate site symmetry and the nature of the hydrogen–substrate interaction [13–15]. A further advantage of neutron scattering in this context is the low absorption in most materials, which facilitates in situ measurements involving cryostats and pressure vessels. These first experiments were performed on as-produced SWNTs that were not purified or processed in a way to produce cutting or opening of tubes, and provide benchmarks for future studies.

2. Experimental procedures

The growth of the crude SWNT sample by laser vaporization was described elsewhere [16]. In brief, we followed Guo et al. [17] but used a single Nd:YAG laser which generated ~450 ns pulses at 1064 nm and 10 Hz at an average power of 20–30 W/cm^2. The power density was selected to operate in a vaporization regime during synthesis [18] to minimize the number of graphite particles which were ejected from the target and incorporated into the vaporized soot. Targets were made by pressing powdered graphite doped with 0.6 at.% each of Co and Ni in a 1–1/8 inch die at 10,000 psi. Crude soot was produced at 1200°C with 500 Torr Ar flowing at 100 sccm. Raw materials were determined to contain ~20–30 wt% SWNTs as well as agglomerates of amorphous and nanocrystalline carbon, and metal nanoparticles [16]. No further processing was performed to purify the soot or to open the tube ends. Neutron powder diffraction data were collected on 0.6 g of

nanotube soot sealed in a vanadium cell. A wavelength of 2.0783(2) Å was selected using a germanium (3 1 1) monochromator with a 75° take-off angle and an in-pile collimation of 15 min of arc. Data were collected over the range of 1.3–166.3° 2θ with a step size of 0.05°.

For hydrogen loading, 0.55 g of the nanotube soot was sealed inside a high pressure aluminum cell, heated to 350 K and placed under dynamic vacuum for ~12 h with a mechanical pump (~10^{-3} Torr). While the temperature and ultimate pressure may not be sufficient to remove all impurities adsorbed during exposure to the atmosphere [1], perfect loading conditions may not be necessary to extract information about the location and environment of the adsorbed hydrogen. Hydrogen gas was introduced directly from a standard cylinder at a pressure of ~11 MPa and the system was isolated to monitor for any pressure leaks over a period of 48 h. To ensure full loading, the sample was cooled in a helium cryostat to 25 K over a period of 18 h while remaining in contact with the hydrogen gas source at 11 MPa. After isolating the hydrogen cylinder, the sample space was evacuated using a mechanical pump for 90 min until evolution of non-adsorbed hydrogen slowed and the vessel pressure was reduced to ~10^{-3} Torr. Neutron energy loss spectra were recorded on heating between 25 and 65 K, with 10 min equilibration time allowed at each temperature. Based on the measured neutron intensity compared to that from a known quantity of H_2 in Na_2C_{60} [19], we estimate the amount of adsorbed hydrogen to be ~0.5 wt% at 25 K.

3. Results

The neutron powder diffraction pattern taken at room temperature is shown in Fig. 1. The pattern is characteristic of nanotube bundles, with four broad features between 5° and ~30° superimposed on an intense background due to small angle scattering [20]. Additional sharp features at higher scattering angles coincide with the predicted peak positions from graphitic carbon (marked by asterisks and also with the (0 0 2) reflection labeled). Weak features that arise from small amounts of fcc

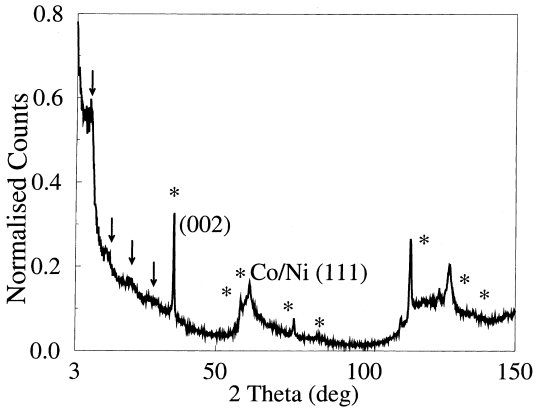

Fig. 1. Neutron powder diffraction pattern of the nanotube soot at room temperature. The pattern covers the range 3–150° in 2θ at a wavelength of 2.0783 Å. The nanotube rope nature of part of the sample is evidenced by the broad low angle reflections indicated with arrows. Asterisks mark graphite reflections with the (0 0 2) labeled. Low catalyst presence is evidenced by low intensity in the nickel (1 1 1) reflection.

Ni (perhaps alloyed with Co) are also present. The four features at low angles correspond well with those of a rope bundle of ~1.4 nm diameter nanotubes in van der Waals contact, forming a hexagonal lattice with $\mathbf{a} = 17$ Å [20]. This is consistent with the SWNT diameters observed by Raman spectroscopy [21]. The peak width of the (0 0 2) graphite reflection corresponds to a coherence length ~100 layers, consistent with a small amount of the graphite ablated from the target during synthesis, and not with the formation of graphitic onions or nanoshells.

Fig. 2 shows the neutron energy loss spectra recorded between 10 and 20 meV at several temperatures between 25 and 65 K on warming. The spectra consist of a single peak at ~14.5 meV, only slightly shifted from the value of 14.7 meV characteristic of unhindered rotations. The peak energy is consistent with similar results for solid hydrogen [22], H_2 adsorbed on graphite [23], and H_2 intercalated into octahedral sites in fcc solid C_{60} [13]. We therefore assign this peak as the $J = 0 \rightarrow 1$ (*para–ortho*) transition in molecular hydrogen which is physisorbed on the exterior surfaces of the nanotubes. At all our measurement temperatures, free hydrogen would be gaseous which would lead to significant recoil effects [24].

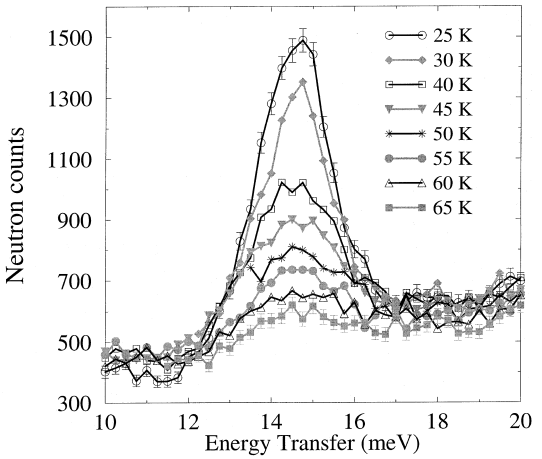

Fig. 2. Temperature dependence of the neutron energy loss spectra for the hydrogen–nanotube system, taken on heating from 25 K. For clarity, only error bars for the 25 and 65 K data sets are plotted.

These would shift and broaden the observed scattering relative to that expected for a free rotor. Because the scattering we observe is only slightly perturbed with respect to the pure solid, the center-of-mass of the hydrogen molecule must be essentially fixed in space. Since our sample was not purified, we must also consider the possible influence of other constituents. Ni and Co are known to dissociate the H_2 molecule, so chemisorbed hydrogen on catalyst particles would not contribute to the rotational transition. We can also rule out a contribution from the graphitic impurities evident in Fig. 1 since H_2 monolayers are liquid-like and unstable on flat graphene surfaces above 20 K [23].

These measurements therefore provide good evidence that molecular hydrogen physisorbs on the curved exterior surface of SWNTs. We collected a full data set over the energy transfer range 6–40 meV at 25 K, and compared this to a spectrum of the pristine soot without hydrogen in the same aluminum can. The only unique feature in the hydrogen-loaded nanotube spectra is the one we assign to the $J = 0 \rightarrow 1$ rotational transition.

Details of the temperature evolution of the $J = 0 \rightarrow 1$ transition were followed by fitting the data to a Gaussian peak with a sloping background function. The temperature variation of the frequency and full-width at half-maximum (FWHM) of the rotational transition are shown in Fig. 3. As previously stated, the average peak frequency of 14.5(1) meV is only marginally reduced from the value found for solid hydrogen. However, the 2.4(4) meV FWHM is over twice as broad as the instrumental resolution ($\sim$1.1 meV). We can infer from the fitted positions that the physisorbed hydrogen is rotationally quite free, with the nanotube–hydrogen interaction potential providing only a small ($<\sim$0.1 kJ/mol) barrier to rotation, in agreement with results for H_2 on graphite [25]. The resolution-corrected FWHM (2.1(4) meV) could be due to symmetry reduction at the hydrogen adsorption sites which would lift the degeneracy of the rotational levels, or it may indicate a distribution of adsorption sites thus a distribution of rotational barrier energies. We note

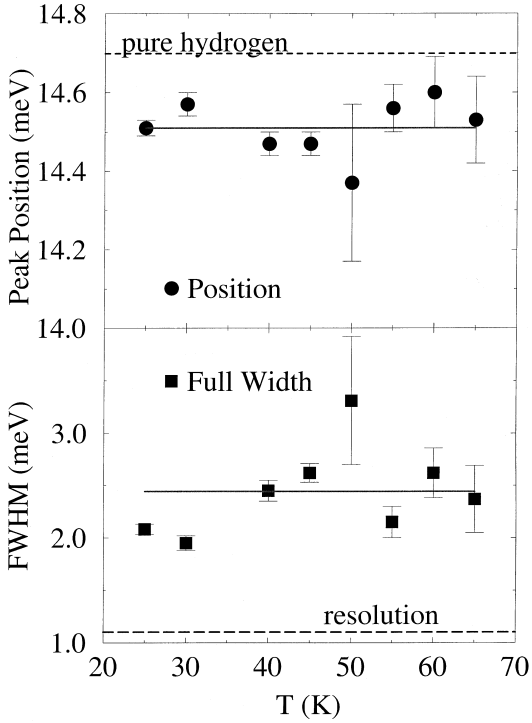

Fig. 3. Fit parameters for the $J = 0 \rightarrow 1$ transitional energy (top, circles) and width (bottom, squares). The solid lines show the average values of the parameters over all temperatures. For comparison, the upper dashed line indicates the transition energy of pure solid hydrogen while the lower dashed line shows the instrumental resolution.

the similarity of these spectra to those obtained for H_2 in C_{60} [13], where the broad $J = 0 \rightarrow 1$ transition was decomposed into two components representing transitions to $M_J = 0$ and $M_J = \pm 1$ sublevels, respectively. In that case, the observed level splitting of $\sim$0.7 meV was attributed to a $\sim$0.1 kJ/mol barrier to rotation, while the slight reduction in transition frequency from 14.7 meV was explained by the large zero-point motion of the hydrogen molecule. It is tempting to make a similar conclusion in this case, though further experiments with higher resolution are required to directly address the origin of the observed line broadening.

While the peak position and width are essentially temperature-independent, the integrated intensity shows an exponential decrease with increasing temperature (not shown), indicating thermally activated desorption of hydrogen from the nanotube surface. This behavior was not observed for H_2 in C_{60}, indicating that the binding energy on SWNT surfaces is significantly less than the value of $\sim$11 kJ/mol for H_2 adsorbed interstitially [13]. Conversely, the binding energy on SWNT must be somewhat greater than on graphite (4 kJ/mol [25]) since the adsorbed H_2 is stable to higher temperatures. We estimate an activation energy of $\sim$6 kJ/mol for our unpurified, unopened SWNTs, with the caveats that the measurements may not have been carried out under equilibrium conditions and the loading conditions may not have been ideal. Nonetheless, the temperature-dependent intensities in the various experiments indicate rather directly that the stability of adsorbed molecular hydrogen increases in the sequence: graphite surface < SWNT material < solid C_{60} with the SWNT binding energy being closer to that of flat graphite than to internal C_{60} cavities. We suggest that the relevant site in the present work is the exterior cylindrical SWNT or bundle surface rather than tube interiors (mainly inaccessible in the present sample) or interstitial channels in the rope lattice (probably more similar to octahedral sites in the fullerene solid). We also attempted to observe the inverse $J = 1 \rightarrow 0$ transition in neutron energy gain with the Fermi-chopper time-of-flight spectrometer at the NCNR, since this would verify our assignment as well as yield information on the rate of *ortho–para* conversion. However, we were unable to observe a peak that could be ascribed to this transition at any temperature. This is likely due to the extremely rapid conversion of all the *ortho* hydrogen to the *para* form via magnetic catalyst particles, resulting in negligible population of the $J = 1$ level. Finally, it should be noted that no scattering which could be attributed to vibrational motions of the H_2 molecules was observed in these measurements. Since one expects to see an in-plane phonon at $\sim$5 meV for a monolayer of H_2 adsorbed on graphite [26,27], this provides further evidence that hydrogen has not been adsorbed onto graphitic impurities. We note, however, that the temperature used in the energy gain experiment may have been too high to observe this mode.

4. Summary

The present neutron energy loss results for the $J = 0 \rightarrow 1$ transition show that the rotational spectrum of hydrogen is only mildly perturbed by association with the nanotubes, similar to what is observed for solid H_2 [20], H_2 on graphite [23], or H_2 in C_{60} [13]. At all temperatures the peak is broadened compared to the instrumental resolution. This is probably due either to a lifting of the degeneracy of the $J = 1$ rotational level by the adsorption site symmetry, or to multiple adsorption sites. The results are reminiscent of those obtained for interstitial hydrogen in C_{60}, where a rotational barrier of $\sim$0.1 kJ/mol was observed. There is an exponential decrease in the intensity of this peak with increasing temperature due to the desorption of the physisorbed hydrogen, indicating a binding energy significantly less than the 19.6 kJ/mol reported for opened SWNTs produced by arc discharge [1]. We conclude that the main binding site under the present loading conditions is the outer surface of isolated tubes and/or tube bundles, with a provisional value for the binding energy of $\sim$6 kJ/mol. These results are valuable as they provide benchmark values to which future hydrogen adsorption experiments on purified and opened SWNTs can be compared.

Acknowledgements

This work was supported in part by the Department of Energy DOE DEFG02-98ER45701 (J.E.F.). The work at NREL was supported by the Office of Science, Basic Energy Sciences, Division of Materials Science and the Office of Energy Efficiency and Renewable Energy Hydrogen Program of the Department of Energy under Grant No. DE-AC36-99GO10337.

References

[1] A.C. Dillon, K.M. Jones, T.A. Bekkedahl, C.H. Kiang, D.S. Bethune, M.J. Heben, Nature 386 (1997) 377.
[2] C. Liu, Y.Y. Fan, M. Liu, H.T. Cong, H.M. Cheng, M.S. Dresselhaus, Science 286 (1999) 1127.
[3] P. Chen, X. Wu, J. Lin, K.L. Tan, Science 285 (1999) 91.
[4] A. Chambers, C. Park, R.T.K. Baker, N.M. Rodriguez, J. Phys. Chem. B 102 (1998) 4253.
[5] C. Park, P.E. Anderson, A. Chambers, C.D. Tan, R. Hidalgo, N.M. Rodriguez, J. Phys. Chem. B 103 (1999) 10572.
[6] Y.Y. Fan, B. Liao, M. Liu, Y.L. Wei, M.Q. Lu, H.M. Cheng, Carbon 37 (1999) 1649.
[7] Y. Ye, C.C. Ahn, C. Witham, B. Fultz, J. Liu, A.G. Rinzler, D. Colbert, K.A. Smith, R.E. Smalley, Appl. Phys. Lett. 74 (1999) 2307.
[8] R.T. Yang, Carbon 38 (2000) 623.
[9] C.C. Ahn, Y. Ye, B.V. Ratnakumar, C. Witham, R.C. Bowman, B. Fultz, Appl. Phys. Lett. 73 (1998) 378.
[10] G. Stan, M.W. Cole, J. Low Temp. Phys. 110 (1998) 539.
[11] J.K. Stalick, et al., Mater. Res. Soc. Symp. Proc. 376 (1995) 101.
[12] J.R.D. Copley, D.A. Neumann, W.A. Kamitakahara, Can. J. Phys. 73 (1995) 763.
[13] S.A. FitzGerald, T. Yildirim, L.J. Santodonato, D.A. Neumann, J.R.D. Copley, J.J. Rush, F. Trouw, Phys. Rev. B. 60 (1999) 6439.
[14] J. Eckert, J.M. Nicol, J. Howard, F.R. Trouw, J. Phys. Chem. 100 (1996) 10646.
[15] A.P. Smith, R. Benedek, F.R. Trouw, M. Minkoff, L.H. Yang, Phys. Rev. B 53 (1996) 10187.
[16] A.C. Dillon, T. Gennett, K.M. Jones, J.L. Alleman, P.A. Parilla, M.J. Heben, Adv. Mater. 11 (1999) 1354.
[17] T. Guo, P. Nikolaev, A. Thess, D.T. Colbert, R.E. Smalley, Chem. Phys. Lett. 243 (1995) 49.
[18] A.C. Dillon, P.A. Parilla, K.M. Jones, G. Riker, M.J. Heben, Mater. Res. Soc. Symp. Proc. 526 (1998) 403.
[19] S.A. FitzGerald, T. Yildirim, L.J. Santodonato, D.A. Neumann, unpublished.
[20] A. Thess, R. Lee, P. Nikolaev, H.J. Dai, P. Petit, J. Robert, C.H. Xu, Y.H. Lee, S.G. Kim, A.G. Rinzler, D.T. Colbert, G.E. Scuseria, D. Tomanek, J.E. Fischer, R.E. Smalley, Science 273 (1996) 483.
[21] A.C. Dillon, P.A. Parilla, J.L. Alleman, J.D. Perkins, M.J. Heben, Chem. Phys. Lett. 316 (2000) 13.
[22] I.F. Silvera, Rev. Mod. Phys. 52 (1980) 393.
[23] M. Nielsen, W.D. Ellenson, in: M. Krusins, M. Vuorio (Eds.), Proceedings of the 14th International Conference on Low Temperature Physics, North Holland, Amsterdam, 1975, p. 437.
[24] J. Tomkinson, Chem. Phys. 127 (1988) 445.
[25] L. Mattera, F. Rosatelli, C. Salvo, F. Tommasini, U. Valbusa, G. Vidali, Surf. Sci. 93 (1980) 515.
[26] M. Nielsen, J.P. McTague, L. Passell, in: J.G. Dash, L. Ruvalds (Eds.), Phase Transitions in Surface Films, Plenum Press, New York, 1980, p. 127.
[27] M. Nielsen, J.P. McTague, W. Ellenson, J. Phys. 38 (1977) C4.